Applied Thermal Engineering 174 (2020) 115340

Contents lists available at ScienceDirect

Applied Thermal Engineering

journal homepage: www.elsevier.com/locate/apthermeng

Intelligent bidirectional thermal regulation of phase change material incorporated in thermal protective clothing

Yun Su[a,b,c,d], Wen Zhu[a], Miao Tian[a,d,*], Yunyi Wang[a,d], Xianghui Zhang[a,d], Jun Li[a,d,*]

[a] College of Fashion and Design, Donghua University, Shanghai 200051, China
[b] Center for Civil Aviation Composites, Donghua University, Shanghai 201620, China
[c] Shanghai Center for High Performance Fibers and Composites, Shanghai 201620, China
[d] Key Laboratory of Clothing Design and Technology, Donghua University, Ministry of Education, Shanghai 200051, China

HIGHLIGHTS

- PCM with bidirectional thermal regulation was designed and fabricated successfully.
- Heat transfer in thermal protective clothing containing PCM layer was investigated.
- Effects of PCM layer on thermal protection and thermal hazard were examined.
- PCM showed great potential applications for intelligent thermal protective clothing.

ARTICLE INFO

Keywords:
Phase change material
Thermal regulation
Thermal protective clothing
Thermal energy storage
Heat release

ABSTRACT

Coating of fabric by organic phase change materials (PCMs) loaded with paraffin wax changed thermal properties of the fabric. The PCM coated fabric with intelligent bidirectional thermal regulation was designed and prepared. The basic and thermal physical properties of the PCM coated fabric were measured. The PCM layer was incorporated into thermal protective clothing, and the thermal protective performance was evaluated under hot contact exposure. High thermal capacity of PCM increased the potential of thermal protective clothing for heat accumulation during the hot contact exposure, but also modified heat release from the thermal protective clothing after the end of exposure. The incorporation of the PCM coated fabric increased greatly the thermal protective performance during the heat exposure, which was influenced by melt temperature, PCM content and enthalphy. The thermal hazardous effect caused by the PCM coated fabric was slightly increased, but presenting no significant correlation with the skin absorbed thermal energy after the exposure. Therefore, the PCM showed great potential applications for developing intelligent thermal protective clothing. The conclusions obtained from this study contributed to development of PCM with high thermal capacity and low heat release suitable for the thermal protective clothing.

1. Introduction

Phase change material (PCM) can absorb, store and release large amounts of latent heat during the process of physical state change from solid to liquid or liquid to gas or vice versa [1,2]. The intelligent thermal regulation properties of PCM are attracting increasing attention to enhance the energy utilization efficiency and the thermal regulation. Microencapsulated PCM possessing excellent capacity of latent thermal energy storage has gained a considerable development in fundamental researches, such as solar-thermal conversion systems [3], thermal energy storage [4,5], encapsulated autonomic healing materials [6,7], photochromic materials [8,9], reversibly thermochromic materials [10]. In recent decades, carbon black loaded organic phase change material was developed to enhance thermal conductivity and photothermal efficiency and identify a promising application in latent heat thermal energy storage [11,12].

Various types of PCMs have long been used in clothing as a means of body heat regulation for comfort enhancement, such as sportswear for ice climbing, space suits and gloves. These materials absorb the heat generated by a human body during action and release the heat when cooled. More recently, microencapsulated PCMs have seen application in textile design for energy absorbing clothing for thermal hazardous

* Corresponding authors.
E-mail addresses: tianmiao@dhu.edu.cn (M. Tian), lijun@dhu.edu.cn (J. Li).

https://doi.org/10.1016/j.applthermaleng.2020.115340
Received 10 January 2020; Received in revised form 26 March 2020; Accepted 12 April 2020
Available online 14 April 2020
1359-4311/

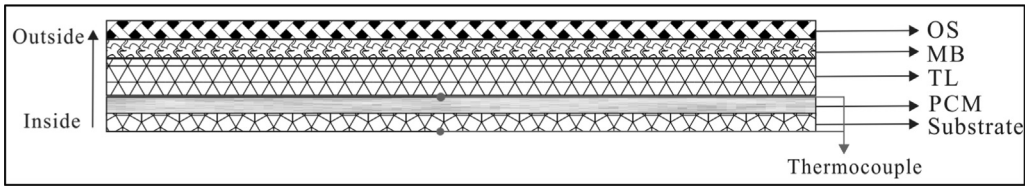

Fig. 1. Distribution of different layer fabrics for thermal protective clothing.

environments, such as flash fire, thermal radiation, and thermal convection [13–18]. Zhao et al. [13] investigated the effect of the incorporated PCM layer on thermal protective performance of firefighting protective clothing. The impregnation of cotton fabric by the PCM increased the thermal energy storage, thus improving the thermal protective performance. The influences of basic properties of PCM on the thermal protective performance, such as mass, melt temperature and entrapping position, were further examined under low-level, medium-level and high-level thermal radition [14–16,19]. Geng et al. [20] prepared a series of reversible thermochromic microencapsulated PCMs with excellent latent heat storage-release performance, and showing great potential in thermal protective clothing. In addition, Wan et al. [16] designed a new cooling garment equiping with PCMs and ventilating fan that greatly improved human thermal comfort in hot environment.

The PCM presents a process of heat charging and discharging cycle [21]. The absorb of thermal energy in the PCM during the heat exposure is the charging process, while the discharge of thermal energy after the heat exposure is the discharging process. However, these studies ignored the effect of discharge of thermal storage in the PCM on human safety. Some studies in recent years reported that the thermal protective clothing exerted the thermal hazardous effect on wearer when it should be providing the thermal protection [22]. This was due to the fact that the thermal energy stored in the clothing was discharged to the human body after the exposure, thus exacerbating skin burn injury [23,24]. The discharging of stored thermal energy in the clothing was demonstrated to be related to fabric thickness, density, thermal capacity, air gap size, moisture content and applied pressure to the fabric [23–26]. The incorporation of PCMs increased the stored thermal energy in the clothing, which could enhance the thermal hazardous effect. Thus, the thermal hazardous effect of the PCMs should be further investigated for comprehensively assessing the application of PCMs in the thermal protective clothing.

Additionally, the previous studies applied the PCMs to the thermal protective clothing exposing to flame and thermal radiation exposures. There existed few studies regarding the incorporation of PCMs in the thermal protective clothing exposed to hot contact surface. Reports on the etiology of injuries to firefighters indicate that about 15% of injured firefighters received contact or compression burns [27]. The clothing under the hot contact exposure was compressed, thus affecting the thermal physical properties and heat transfer of clothing. Convective and radiative heat transfer were the dominant heat transfer mode for flame and thermal radiation exposures, while the thermal energy was mainly transferred by conduction for the hot contact exposure. Therefore, it was crucial to examine the influence of PCM on the conductive heat transfer under the hot contact exposure.

The objective of the study was to obtain the most suitable PCM for increasing the thermal protective performance and decreasing the thermal hazardous effect of clothing. The paper presented the microencapsulated PCMs with four kinds of melt temperatures that were coated to a flame-resistant fabric. Thermal physical properties for the PCM coated fabric were measured. The PCM layer was entrapped into the thermal protective clothing, exposing to the hot contact surface. The effect of PCM layer on the heat transfer in the clothing were investigated. The bidirectional thermal regulation for the PCM layer was analyzed in detail. The finding obtained from this study contributed to development of intelligent thermal protective clothing for increasing the thermal comfort of firefighter and decreasing the skin burn due to overheating.

2. Materials and methods

2.1. Materials

2.1.1. PCM

Paraffins are commonly used for clothing thermal regulation due to their compatibility, nonsupercooling, and high heat storage capacity. The paraffin was enclosed in microcapsule for greatly decreasing the leakage. In this study, four types of paraffins with different melt temperatures (25 °C, 30 °C, 35 °C, 42 °C) were selected. These melt temperatures were less than the temperature of skin burn threshold (44 °C) for absorbing more thermal energy before the skin burn, thus minimizing the skin burn [28].

2.1.2. Thermal protective clothing

Thermal protective clothing is commonly comprised of an outer shell (OS), a moisture barrier (MB) and a thermal liner (TL). The PCM was coated to a flame-resistant fabric (substrate) as a PCM layer that was entrapped into the innermost layer of thermal protective clothing (see Fig. 1). The basic specifcations are listed in Table 1. The mass per unit area was tested based on an electronic scale tester, conformed with standard ASTM D3776-96. In accordance with standard ASTM D1777-96, the thickness of test specimen was measured under a pressure of 1 kPa. The air permeability of the PCM coated fabric was measured under a pressure drop of 200 Pa using a Frazier Air Permeability Tester, according to EN ISO 9237.

2.2. Preparation of PCM coated fabrics

For preparing uniform and stable PCM coated fabric, a process flow diagram is designed in Fig. 2. The substrate needed to be well-pressed before use. The coating slurry was prepared by mixing microcapsule suspension, thickner, adhesive and water. The thickner (HEUR-B) was used to mix all components for speeding up the uniform dispersion and maintaining the surface smooth. The percentages of these components were different in the coating slurry, as listed in Table 2. The coating

Table 1
Basic properties of single-layer fabric.

Fabric type	Fiber content	Fabric structure	Mass (g/m^2)	Thickness (mm)	Air permeability (mm/s)
OS	Nomex IIIA	Twill	164	0.32	195.9
MB	Nomex/Kevlar (PTFE)	Hydroentanglement felt with PTFE	112	0.55	1.2
TL	100% Meta-aramid + 50% Nomex/50% flame-resistant viscose	Needle-punched nonwoven + plain	143	1.66	1034.8
Substrate	Nomex IIIA	Twill	229	0.49	81.8

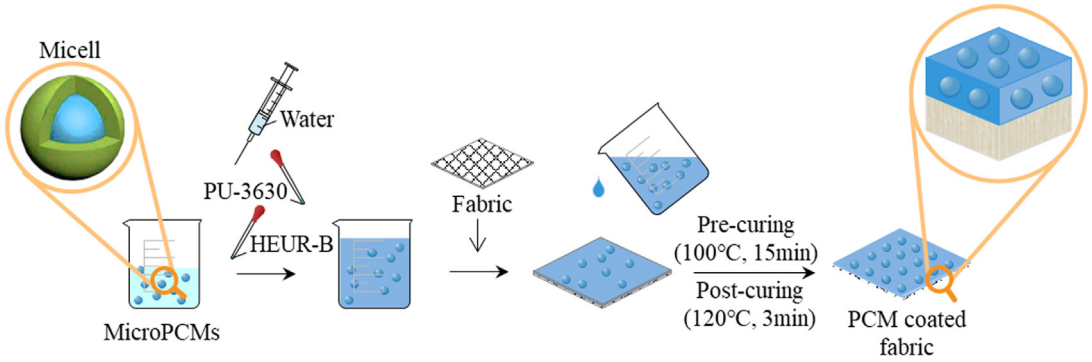

Fig. 2. Formation process of PCM coated fabric.

Table 2
Coating slurry with different contents of PCM.

Number	Phase change temperature (°C)	PCM content	Moisture content
PCM-25a	25	25%	55%
PCM-25b	25	35%	45%
PCM-25c	25	45%	35%
PCM-30a	30	25%	55%
PCM-30b	30	35%	45%
PCM-30c	30	45%	35%
PCM-35a	35	25%	55%
PCM-35b	35	35%	45%
PCM-35c	35	45%	35%
PCM-42a	42	25%	55%
PCM-42b	42	35%	45%
PCM-42c	42	45%	35%

slurry was coated onto the surface of substrate by using a Rapid laboratory coating machine (Werner Mathis AG, Switzerland). Fabric specimens were coated by taking different amounts of PCM at a constant machine setting, as shown in Table 2. The thickness and the mass of coated fabric were used for quantitatively evaluating the uniform dispersion. The coated fabric was pre-heated at 100 °C for 15 min and then dried at 120 °C for 3 min. The coated fabric was required to be placed in drying oven for 24 h. The moisture in the coated fabric was evaporated completely in the drying process.

2.3. Methods

2.3.1. Measurement of basic properties

The basic properties of the PCM coated fabric are listed in Table 3. The mass per unit area (substrate and PCM), thickness, air permeability of the PCM coated fabric were measured according to the mentioned methods in the Section 2.1.2. Breaking strengths in warp and weft of the PCM coated fabric were tested by an electronic universal testing machine (model INSTRON-6025). The mechanical strength for the PCM coated fabric was marginally larger than no coated fabric, while the coating technique sharply decreased the air permeability. This indicated that the coating did not significantly affect the mechanical properties of substrate fabric.

2.3.2. Measurement of thermal physical properties

(1) Coefficient of thermal conductivity

Table 4 shows the thermal conductivity of the PCM coated fabrics. The thermal conductivity of textile fabric is widely determined under a steady-state heat flux by a guarded-hot-plate apparatus (KESF-TLII). The test apparatus is comprised of a hot plate, a guard heater, and a cold plate. According to standard ASTM D1518-2014, the hot and cold plates maintained the boundary conditions constants (35 and 25 °C) in the superior and inferior surfaces of specimen. In the ideal case, the plates were in perfect thermal contact with the specimen and the heat flow through it was one-dimensional and independent of time. The heat flow was from the hot plate to the cold plate along the direction of specimen thickness. Under these conditions, the apparent thermal conductivity (λ) of the PCM coated fabrics was determined from the heat flux (q) through it, the temperature difference ($T_h - T_c$) between the hot and cold plates, and the thickness (L) of the PCM layer, written as:

$$\lambda = \frac{qL}{A(T_h - T_c)} \quad (1)$$

Table 3
Basic properties of PCM coated fabrics.

PCM number	Mass per unit area (g/m^2)	Thickness (mm)	Air permeability (mm/s)	Breaking strength	
				Warp	Weft
PCM0	229 (2)	0.49 (0.01)	81.8 (2.5)	1494 (117)	1000 (59)
PCM-25a	522 (10)	0.70 (0.02)	0.0 (0.0)	1616 (27)	1185 (8)
PCM-25b	539 (6)	0.74 (0.02)	0.0 (0.0)	1635 (14)	1147 (43)
PCM-25c	550 (43)	0.80 (0.04)	0.0 (0.0)	1643 (17)	1183 (21)
PCM-30a	454 (2)	0.74 (0.02)	0.0 (0.0)	1628 (21)	1121 (12)
PCM-30b	497 (11)	0.73 (0.02)	0.0 (0.0)	1646 (30)	978 (15)
PCM-30c	493 (7)	0.76 (0.02)	0.0 (0.0)	1581 (30)	1172 (33)
PCM-35a	462 (6)	0.75 (0.04)	0.1 (0.2)	1622 (21)	1155 (11)
PCM-35b	515 (11)	0.78 (0.04)	0.0 (0.0)	1615 (23)	1136 (12)
PCM-35c	521 (7)	0.79 (0.02)	0.0 (0.1)	1625 (10)	1093 (19)
PCM-42a	451 (8)	0.72 (0.03)	0.0 (0.0)	1611 (15)	1132 (12)
PCM-42b	459 (2)	0.70 (0.04)	0.0 (0.0)	1602 (32)	1165 (16)
PCM-42c	504 (9)	0.73 (0.04)	0.0 (0.0)	1551 (30)	1171 (17)

Note: the value in the bracket is standard error.

Table 4
Thermal physical properties of the PCM coated fabric.

PCM number	Melt temperature range (°C)	Peak temperature (°C)	Phase-transition enthalpy (J/g)	Thermal conductivity (W/(m·K))
PCM0	–	–	–	0.050
PCM-25a	9.0–34.2	26.4	46.7	0.071
PCM-25b	8.8–33.7	26.7	46.9	0.086
PCM-25c	9.2–40.0	26.6	63.9	0.077
PCM-30a	23.4–40.2	33.3	106.7	0.094
PCM-30b	21.3–42.4	35.2	120.6	0.083
PCM-30c	20.4–41.2	33.3	114.9	0.080
PCM-35a	32.5–52.5	43.3	63.9	0.074
PCM-35b	29.2–50.1	41.1	104.5	0.072
PCM-35c	28.6–52.3	41.5	144.9	0.075
PCM-42a	34.0–52.8	45.5	86.0	0.072
PCM-42b	33.3–55.3	45.6	100.6	0.072
PCM-42c	34.5–55.8	47.1	107.0	0.067

where A is the area of the hot plate (0.0025), m^2.

(2) Melt temperature and latent heat

Differential scanning calorimetry (DSC) is commonly used to determine latent heat, melt range and specific heat. The test apparatus consists of three different main components: the instrument itself containing all the system electronics, the cell monitoring the heat flow and temperature, and the cooling accessory. The DSC was purged with dry nitrogen throughout the experiment. The empty specimen holder, the sapphire standard and the specimen holder plus lid were weighed, respectively. The same reference specimen holder plus lid were used for the sapphire standard run and for the test specimen run. The DSC test chamber was cooled, and maintained isothermally at the temperature of −20 °C for at least 4 min to establish equilibrium. The test specimen was heated from the initial to final temperature (80 °C) at a rate of 10 °C/min. The thermal curve during the heating phase was continually recorded, and a steady-state isothermal baseline at the upper temperature limit was recorded. Based on the thermal curve, the enthalpy of phase change and specific heat capacity were calculated. The calculated equations were obtained from standard ASTM E1269. Table 4 lists the enthalpy and the melt range for different PCM contents and melt temperatures.

2.3.3. Evaluation of thermal protective performance against hot surface contact

A bench top tester was used to assess the thermal protective performance of fabric system incorporating the PCM layer against hot surface contact, as shown in Fig. 3 [29]. The test apparatus is comprised of a heat source, a specimen fixed component, a pressure controller and a data acquisition system. The heat source includes a hot plate and a surface plate (aluminium) with a wide of 140 by 140 mm. The hot plate with a controlled temperature was employed to simulate hot object hazards due to contact or compression. The pressure controller was connected to an air pump for regulating the applied pressure to the specimen. Skin-simulant sensor behind the specimen was used to record the change of skin temperature as the sensor housing is construct of Macor®, an inorganic material having similar thermal physical properties with human skin. The skin-simulant sensor enclosing with the specimen was moved up and down under the driving force of air pump. The test specimen was insulated from the hot plate by using a heat insulation plate for ceasing the exposure, which aimed to ensure the heat exposure duration.

The developed test apparatus is required by standard ASTM F1060. The thermal protective performance test was conducted in a climate chamber with 25 °C temperature and 65% relative humidity. According to the standard ASTM F1060, the exposure intensity was calibrated

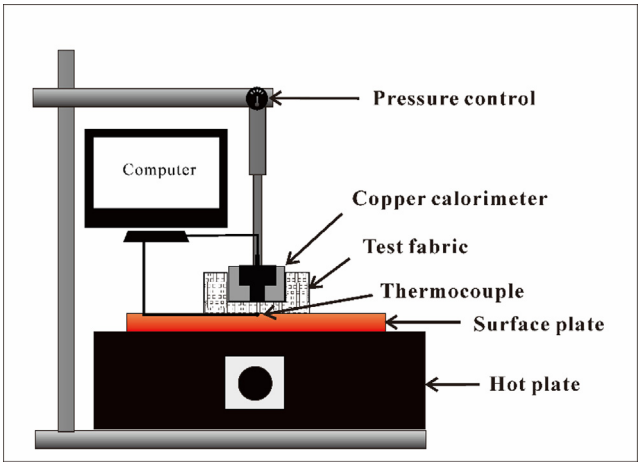

Fig. 3. Schematic diagram of thermal protective performance tester.

before mounting the testing sample. The hot plate required at least 15 min to reach a required temperature of 316 °C. After completing the calibration, the skin-simulant sensor and the test specimen were moved down for initialing the heat exposure. The heat exposure time was 60 s. After the heat exposure of 60 s, the copper calorimeter and the test specimen were moved up, and the temperature data was recorded continually for 540 s as a cooling phase. In addition, the temperature changes on the PCM layer were measured by T-type thermocouple with a diameter of 0.1 mm (OMEGA, Engineering, USA) (see Fig. 1). The thermocouple attachment method was described in detail in Lawson's study [30]. Each specimen was tested three times and the average value was calculated.

The temperature on the skin-simulant sensor was input to skin bio-heat transfer model for calculating the skin temperature in deeper-layer tissues. The heat transfer within the skin tissues was assumed as a transient one-dimensional heat diffusion problem. According to standard ASTM F1930-18, the skin bio-heat transfer model that considered the enhanced heat transfer due to changing blood flow in the dermis and subcutaneous layers is written as,

$$(\rho c_p)_{skin}\frac{\partial T}{\partial t} = \frac{\partial}{\partial x}\left(k_{skin}\frac{\partial T}{\partial x}\right) + w_b(\rho c_p)_b(T_b - T) \quad (2)$$

where ρ_{skin} and $(c_p)_{skin}$ are the density and specific heat of each layer skin tissue, ρ_b and $(c_p)_b$ are the density and specific heat of blood, respectively, w_b is the rate of blood perfusion at dermis layer and subcutaneous tissue, and T_b is the blood temperature. The properties and parameters of each skin layer in skin heat transfer model were obtained from standard ASTM F1930-18.

The temperature histories versus time in different skin layers were calculated by the equation (2). Skin burn injury could take place when the basal layer or the dermal layer temperature reached 44 °C [27]. Henriques burn integral model was employed to predict 2nd and 3rd degree skin burns, given by,

$$\Omega = \int_0^t P\exp(-\frac{\Delta E}{RT})dt \quad (3)$$

where Ω is a quantitative measure of burn damage at the basal layer or at any depth in the dermis, R is the universal gas constant, T is the absolute temperature at the basal layer or at any depth in the dermis, and t is the total time for which T is above 44 °C. The temperatures of more than 44 °C at the epidermis–dermis interface and the dermis–subcutaneous tissue interface were input into the equation (3) to calculate the burn damage (Ω). These constants for calculation of Ω could be obtained in ASTM F2731-11. When the Ω reaches a value of 1 at the epidermis–dermis interface and the dermis–subcutaneous tissue interface, the corresponding times are treated as 2nd and 3rd degree burn times, respectively. The predicted skin burn times were used to evaluate

the thermal protective performance of the fabric under hot surface contact.

2.3.4. Calculation of stored and discharged thermal energy

The performance of bidirectional thermal regulation of PCM layer includes the thermal protective performance and the thermal hazardous effect. In this study, the stored thermal energy during the exposure and the time to skin burn was used to assess the thermal protective performance of the PCM layer. The transferred thermal energy to skin after the exposure was used to evaluate the thermal hazardous effect of clothing.

The heat flux through the test specimen ($q(t)$) was calculated by the temperature changes on the sensor's surface according to Duhamel's theorem, written as,

$$q(t) = \sqrt{\frac{k\rho c_p}{\pi}}\left(\frac{1}{2}\int_0^t \frac{\mathrm{T}_s(t) - \mathrm{T}_i}{t^{\frac{1}{2}}}\right) \tag{4}$$

where ρ, k and c_p are the density, thermal conductivity and specific heat of the skin simulant sensor, respectively, T_i is the initial temperature on the sensor's surface, and $T_s(t)$ is the transient temperature versus time t on the sensor's surface. The absorbed thermal energy by skin (Q_{sk}) is written as,

$$Q_{sk} = \sum_0^t q(t)\Delta t \tag{5}$$

where $\triangle t$ is the time difference.

The stored and discharged thermal energy in the PCM layer due to the sensible heat was calculated by the temperature changes on the PCM layer, written as,

$$Q_{SH}(t) = \rho_{pcm} c_{pcm} L_{pcm} \frac{\Delta T_1(t) + \Delta T_2(t)}{2} \tag{6}$$

where $Q_{SH}(t)$ is the accumulative stored thermal energy, ρ_{pcm} and c_{pcm} are the density and specific heat of the skin simulant sensor, respectively, L_{pcm} is the thickness of the PCM layer, $\triangle T_1(t)$ and $\triangle T_2(t)$ are the temperature difference at different times for both sides of PCM layer, respectively.

The latent thermal energy ($Q_{LH}(t)$) for the PCM layer could be calculated by the phase-transition enthalpy (E_{pcm}) and the mass of PCM (m_{pcm}).

$$Q_{LH}(t) = m_{pcm} E_{pcm} \tag{7}$$

3. Results and discussion

3.1. Effect of PCM on thermal protective performance

The effect of the PCM layer on the thermal protective performance was examined firstly before analyzing the thermal regulation performance. Fig. 4 shows second-degree skin burn times with different PCM contents and melt temperatures. It was clear that the second-degree skin burn time for these coated fabrics ranged from 25.5 s to 31.8 s. The average value (29.3 s) of the second-degree skin burn time was 66% greater than non-coated fabric (17.7 s). This implied that the incorporation of PCM layer greatly improved the thermal protective performance under the hot contact exposure.

In addition, it was observed that the time to casue second-degree skin burn increased with the PCM content for the same melt temperature. The correlation coefficient between the time to skin burn and the PCM content was 0.651 ($p < 0.05$), indicating a statistically positive correlation. The PCM layer with higher PCM content stored more thermal energy. For the same PCM content, the PCM layer with melt temperature of 35 °C provided the highest thermal protective performance, and secondly was the PCM layer with melt temperature of 42 °C. The time to skin burn presented a significant correlation with the

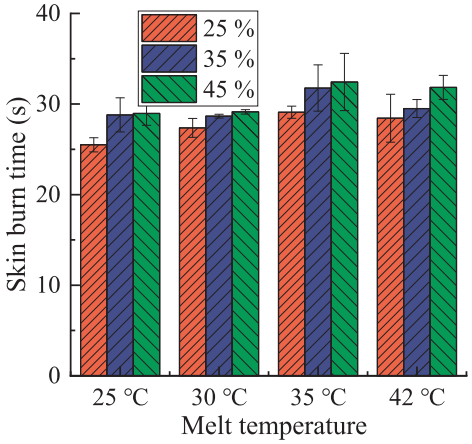

Fig. 4. Second-degree skin burn times for different PCM contents and melt temperatures.

enthalpy of phase change ($r = 0.602$, $p < 0.05$). The rising of the enthalpy could increase the thermal protective performance. Therefore, the PCM layer with melt temperature of 35 °C and 45% PCM content was the most suitable for incorporating into the thermal protective clothing. The increases of the PCM content and the enthalpy could further improve the thermal protective performance. The melt temperature of PCM presented no significant correlation with the skin burn time.

3.2. Effect of PCM on heat transfer through thermal protective clothing

The skin burn times for all samples occurred in heat exposure phase. The PCM layer only absorbed thermal energy during the phase. Thus, it was hard to analyze the effect of heat release from the PCM layer on the skin burn. For analyzing the combined effects of stored and released thermal energy, Fig. 5 shows the temperature changes on the outer surface of PCM layer and the skin surface. It was clear that the temperatures of the PCM layer and the skin surface increased rapidly during the heat exposure, and then decreased substantially after the exposure. For different contents of PCM, the temperatures for the PCM layer at the end of heat exposure (60 s) ranged from 138.6 to 187.8 °C. The temperatures on the skin surface at the 60 s were in between 53.4 and 56.1 °C. With regard to non-coated fabric, the temperatures of the fabric layer and the skin surface increased to 157.1 and 75.6 °C, respectively. The temperature of the skin surface was around 20 °C higher for non-coated fabric. This indicated that the incorporation of the PCM layer obviously decreased the heat transfer through the thermal protective clothing. The PCM layer absorbed a large amount of thermal energy through solid-liquid transition, thus reducing the thermal energy transferring to the skin surface and the skin temperature. However, more thermal energy in the PCM layer was absorbed during the exposure comparing to the non-coated fabric, thus increasing the temperature of the PCM layer. Therefore, the temperatures for these PCM layers (30, 35 and 42 °C melt temperatures) were higher than that for non-coated fabric (see Table 5). The PCM layer with phase change temperature of 25 °C demonstrated an opposite trend. The reason might be that the phase change initialed before the heat exposure, and the PCM layer stored thermal energy from the surrounding environment (not from the hot surface). Thus, the PCM layer with phase change temperature of 25 °C could stored less thermal energy during the exposure comparing to these PCM layers with different phase change temperatures.

After the exposure, the PCM layer could discharge the stored thermal energy to the skin surface for slowing down the temperature drop. It was found that the skin temperature for the non-coated fabric decreased by 20.1 °C from 60 to 120 s. In the same duration, the 4.1 °C

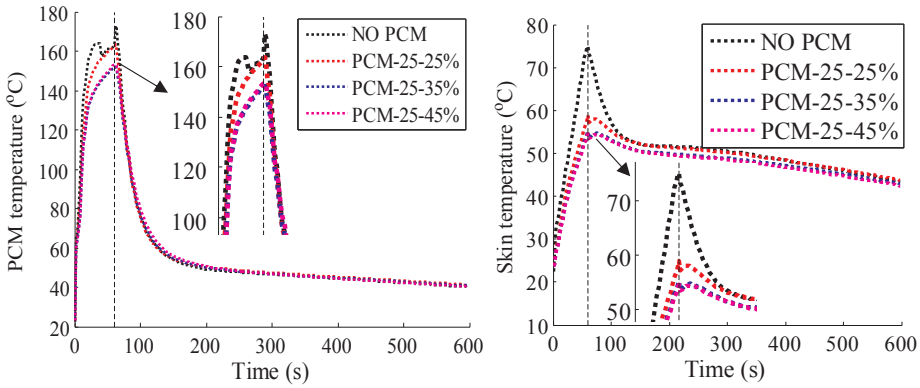

Fig. 5. Changes in PCM temperature and skin temperature with PCM content.

Table 5
Temperature changes in PCM layer and skin surface.

Fabric system	Temperature changes (0–60 s) °C		Temperature changes (60–600 s) °C	
	PCM layer	Skin surface	PCM layer	Skin surface
NO PCM	140.0	52.3	−122.6	−31.5
PCM-25-25%	139.0	34.8	−121.2	−14.9
PCM-25-35%	128.2	31.3	−111.0	−12.1
PCM-25-45%	130.1	31.1	−112.8	−12.3
PCM-30-25%	173.4	33.3	−157.7	−14.8
PCM-30-35%	155.2	32.3	−140.0	−14.9
PCM-30-45%	123.3	32.7	−108.3	−15.9
PCM-35-25%	148.6	32.7	−134.8	−14.5
PCM-35-35%	144.1	31.2	−129.1	−13.8
PCM-35-45%	169.7	31.9	−153.9	−13.8
PCM-42-25%	165.0	33.8	−148.3	−14.8
PCM-42-35%	175.8	33.4	−159.9	−14.0
PCM-42-45%	153.9	30.3	−142.0	−14.0

Note: Positive value indicates the temperature rise; Negative value indicates the temperature drop.

decline was the biggest drop in the skin temperature for the PCM layer. The decline rate for the non-coated fabric was significantly greater than the PCM coated fabrics. This indicated that the releasing thermal energy from the PCM layer decreased the skin cooling at the initial moment of cooling phase. However, the skin temperature for the non-coated fabric was still higher than 50 °C at the 300 s, while the skin temperature was lower than 50 °C for all PCM coated fabrics. It was deduced that the skin cooling was quicker for the fabric system containing the PCM layer with the rising of cooling time.

Fig. 6 shows the effect of melt temperature on PCM temperature and skin temperature. The skin temperature for the non-coated fabric was still far more than that for the PCM coated fabrics. However, the skin temperatures for all PCM layers were approximately equal. This indicated that the change of melt temperature did not affect significantly the skin temperature. The PCM temperature presented a great difference with the rising of melt temperature. The PCM layer with melt temperatures of 35 and 42 °C presented higher PCM temperature, which was related to the thermal conductivity and the melt temperature. Because more thermal energy was stored in the PCM layer with melt temperatures of 35 and 42 °C, thus increasing the temperature of the PCM layer.

In addition, Table 5 listed the temperature changes in the PCM layer and the skin surface during and after the heat exposures. For examining the effects of melt temperature and PCM content on the temperature change, the correlation analysis was conducted in statistic. The temperature change of the PCM layer during the heat exposure presented a highly positive correlation with the melt temperature ($r = 0.645$, $P < 0.05$). Besides, the increased melt temperature significantly enhanced the temperature changes after the exposure ($r = 0.682$, $P < 0.05$). However, there had no obvious correlation between the temperature change of skin surface and the melt temperature. This was because the capacity of storing thermal energy for the PCM layer was determined by many factors, such as enthalphy of phase change, melt temperature and PCM content. Besides, the melt temperature did not increase the enthalphy of phase change according to the Table 4.

The PCM content exterted an important effect on the temperature change of PCM layer during the exposure, but there had no linear correlation between them. The temperature change on the skin surface during the exposure decreased significantly with the PCM content ($P < 0.05$). After the exposure, it was found that the temperature changes for the PCM layer and the skin surface both showed a decrease

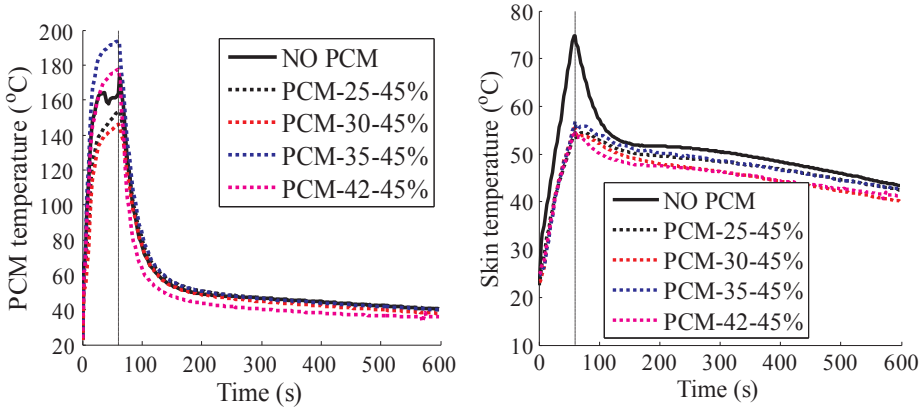

Fig. 6. Changes in PCM temperature and skin temperature with melt temperature.

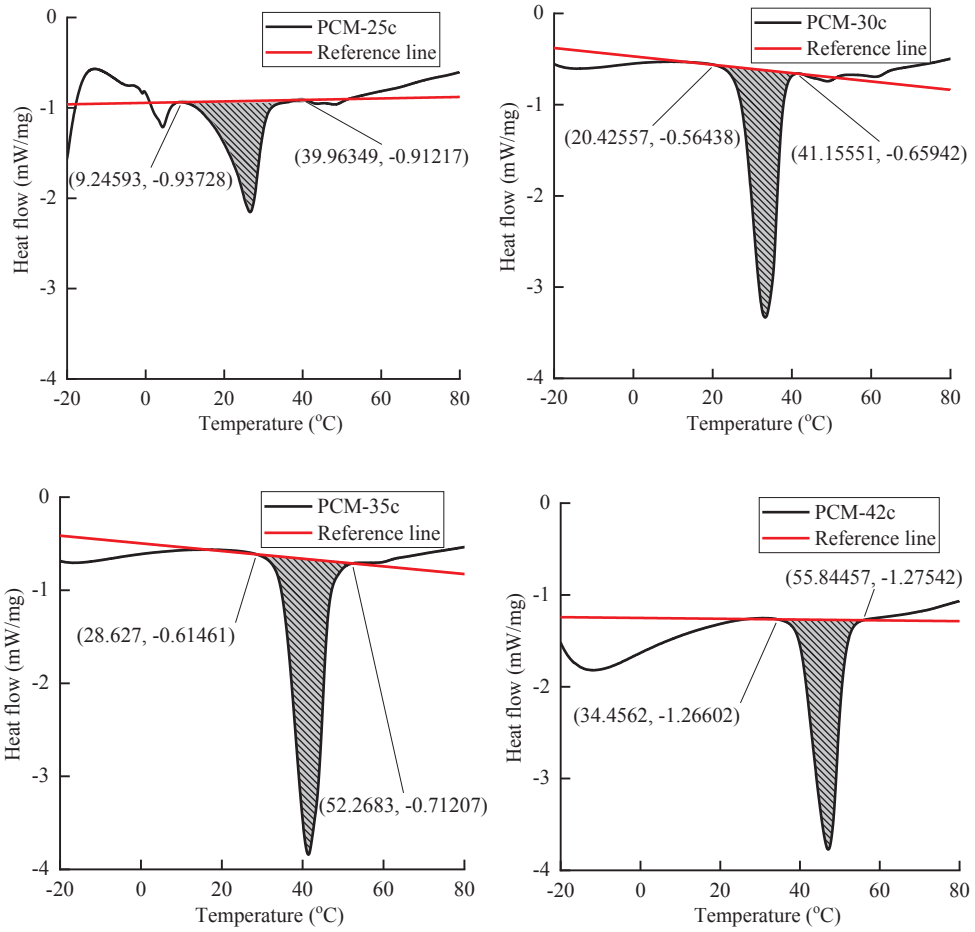

Fig. 7. Thermal curves with different melt temperatures under 45% PCM content.

over the rising of PCM content. This was because that the larger PCM content could increase the stored thermal energy, thus decreasing the thermal energy transferred to the skin surface.

3.3. Bidirectional thermal regulation of PCM

The Section 3.2 discussed the effect of PCM layer on the heat transfer through the fabric system. For further analyzing the bidirectional thermal regulation of PCM, the thermal curves with temperature for the PCM layer are showed in Fig. 7. It was clear that each thermal curve had an endothermic peak (or called mushy zone). The initial and end points of endothermic peak are inflection points, which indicates the initial and end of phase change. The reference line was obtained by connecting initial and end points of endothermic peak. The dash area of the endothermic peak under the reference line was used to calculate the enthalpy of phase change.

For example, the endothermic peak for the PCM layer with 25 °C melt temperature ranged from 9.2 to 40.0 °C, which means the occurance of solid-liquid phase change in the melt range. The lowest point for the endothermic peak indicated the largest rate of absorbed heat, corresponding to the temperature of 26.6 °C. In addition, there existed other endothermic peak before 9.2 °C that was called the phase transition of solid-solid. Thus, the PCM layer with melt temperature of 25 °C might not stored much heat in the heat exposure, since the environmental temperature under the hot contact exposure was around 22 °C. Likewise, the PCM layer with melt temperature of 30 °C initialed to stored heat before the heat exposure, thus decreasing the capacity of storing thermal anergy. The temperature ranges of endothermic peak for melt temperatures of 35 and 42 °C were both more than the initial temperature, meaning that the corresponding PCM layers could absorb more thermal energy under the hot contact exposure.

The endothermic peaks for these PCM layers presented an obvious change with the melt temperature. The increased melt temperature could rise the largest rate of storing heat and the corresponding temperature. The enthalpy of phase change showed an overall increase with the PCM content (Table 4). The enthalpy of phase change for PCM layer of 25 °C melt temperature was lowest in all three kinds of PCM contents, indicating the lowest capacity of storing thermal energy.

The performance of bidirectional thermal regulation includes the thermal protective performance and the thermal hazardous effect. The stored thermal energy during the exposure was used to assess the thermal protective performance of the PCM layer. According to the above results, the stored thermal energy consisting of latent heat and sensible heat for the PCM layer and the skin absorbed thermal energy during the heat exposure were both calculated [17]. It was found that the phase change for all PCMs from the solid to liquid was completed below 60 °C (see Fig. 7). However, the PCM temperature during the exposure was more than 140 °C (see Figs. 5 and 6). Therefore, it was assumed that the PCM was purely liquid during the exposure. The absorbed thermal energy by skin during the exposure was 56.0 J/cm^2 for non-coated fabric, which was far more than the PCM coated fabrics in Fig. 8(b). The PCM layer during the exposure decreased the skin absorbed thermal energy by around 40%. This was because the PCM layer stored the thermal energy due to the sensible heat (SH) and the latent heat (LH). The total stored thermal energy for these PCM layers ranged from 8.9 to 14.89 J/cm^2, which accounted for 26.3% and 46.3% of the skin absorbed energy. As a result, the thermal storage of the PCM layer was extremely important in decreasing the heat transfer to skin.

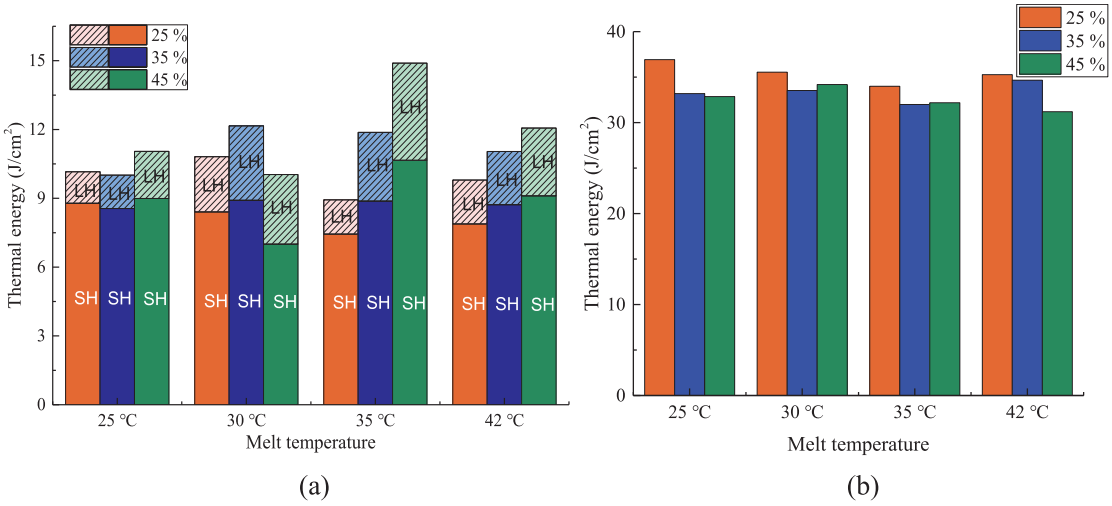

Fig. 8. Thermal energy absorbed by PCM layer (a) and skin layer (b) during the heat exposure.

Moreover, it was found that the stored thermal energy for the PCM layer increased with the PCM content except for the PCM layer with melt temperature of 30 °C. However, the rising of PCM content decreased the absorbed thermal energy by skin. It was deduced that there had a negative relation between the stored thermal energy for the PCM layer and the absorbed thermal energy by skin.

After the heat exposure, the released thermal energy from the PCM layer could quicken up heat transfer and exterted a thermal hazardous effect on human skin. The thermal hazardous effect was analyzed by calculating the skin absorbed thermal energy and the discharged thermal energy from the PCM layer in Fig. 9. The absorbed thermal energy by skin after the exposure was 65.1 J/cm^2 for non-coated fabric, which was slightly less than these PCM coated fabrics (65.4–74.5 J/cm^2). It could be inferred that the incorpation of the PCM layer increased the thermal energy releasing to skin after the exposure.

Fig. 9(a) shows the discharge of thermal energy from the PCM layer. As the temperature of PCM layer at the end of heat exposure was more than 40 °C, the phase change from liquid to solid was not actuated for most of PCMs. Therefore, the released thermal energy included sensible heat and latent heat. The released thermal energy presented a positive correlation with the stored thermal energy, indicating that the more stored thermal energy would result in more heat release. However, the skin absorbed thermal energy showed a decrease with the PCM content, and had a conflict relation with the released thermal energy. The reason might be that the released thermal energy accounting for 9.6% to 14.0% of total skin absorbed thermal energy was simultaneously transmitted to the outer environment and the skin surface. Besides, the PCM layer with larger thermal conductivity increased the cooling rate of skin. Therefore, the release of thermal energy from the PCM layer could aggravate the thermal hazardous effect, but had no significant correlation with the skin absorbed thermal energy.

4. Conclusions

Heat transfer in the PCM layer due to the bidirectional thermal regulation (stored and discharged thermal energy) was obviously distinct from the traditional thermal protective fabrics. During the exposure, the PCM layer for different PCM contents could absorb thermal energy of 8.9–14.89 J/cm^2 through the sensible and latent heat. The skin absorbed thermal energy due to the incorporation of the PCM layer was decreased by around 40%. Therefore, the incorporation of the PCM layer greatly improved the thermal protective performance under hot surface exposure that was related to PCM content, enthalphy and melt temperature.

After the exposure, the PCM layer became a passive heat source that could discharge the thermal energy to the skin surface. The thermal

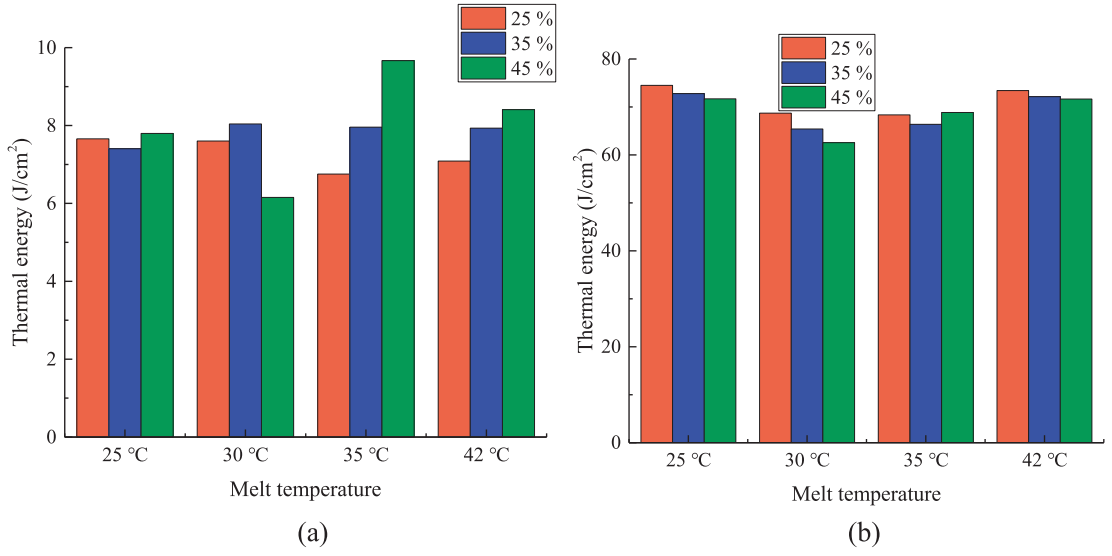

Fig. 9. Thermal energy released by PCM layer (a) and absorbed by skin layer (b) after the heat exposure.

energy of only 6.15–9.67 J/cm^2 was discharged from the PCM layer, which accounted for 9.6 − 14.0% of total thermal energy absorbed by skin. As the discharged thermal energy was simultaneously transmitted to the outer environment and the skin surface, the incorporation of the PCM layer decreased the skin cooling rate mainly in the initial of cooling phase. The PCM layer slightly aggravated the thermal hazardous effect on a human body, but presenting no significant correlation with the skin absorbed thermal energy.

The PCM layer with melt temperature of 35 °C and 45% PCM content was the most suitable for incorporating into the thermal protective clothing, which was influenced by melt temperature, PCM content and enthalphy. The findings obtained from this study contributed to further development of PCM used for thermal protective clothing. However, four kinds of melt temperature and three kinds of PCM content were selected in this study, which caused difficulties in quantitatively analyzing the optimum parameter of PCM. More experimental specimens should be prepared and heat tranfer model in the intelligent thermal protective clothing should be developed to obtain the optimum design parameter of PCM. Furthermore, the thermal protective clothing incorporating the PCM layer should be developed to conduct a human trial, thus further investigating clothing thermal comfort, ergonomics, and durability.

Declaration of Competing Interest

The authors declare that they have no known competing financial interests or personal relationships that could have appeared to influence the work reported in this paper.

Acknowledgement

This work was sponsored by Shanghai Sailing Program (19YF1400600), Open Fund of Shanghai Center for High Performance Fibers and Composites, Fundamental Research Funds for the Central Universities of China (2232019D-18, 2232017D-22 and 2232020G-08), and Humanities and Social Science Fund of Ministry of Education of China (20YJC760087).

Appendix A. Supplementary material

Supplementary data to this article can be found online at https://doi.org/10.1016/j.applthermaleng.2020.115340.

References

[1] K. Pielichowska, K. Pielichowski, Phase change materials for thermal energy storage, Prog. Mater Sci. 65 (2014) 67–123.
[2] A. Sharma, V.V. Tyagi, C.R. Chen, D. Buddhi, Review on thermal energy storage with phase change materials and applications, Renew. Sustain. Energy Rev. 13 (2009) 318–345.
[3] Z. Zheng, Z. Chang, G.-K. Xu, F. McBride, A. Ho, Z. Zhuola, M. Michailidis, W. Li, R. Raval, R. Akhtar, Microencapsulated phase change materials in solar-thermal conversion systems: understanding geometry-dependent heating efficiency and system reliability, ACS Nano 11 (2017) 721–729.
[4] Y.T. Huang, H. Zhang, X. Wan, D. Chen, J. Tang, Carbon nanotube-enhanced double-walled phase-change microcapsules for thermal energy storage, J. Mater. Chem. A 5 (2017) 7482–7493.
[5] T. Nomura, N. Sheng, C. Zhu, G. Saito, D. Hanzaki, T. Hiraki, T. Akiyama, Microencapsulated phase change materials with high heat capacity and high cyclic durability for high-temperature thermal energy storage and transportation, Appl. Energy 188 (2017) 9–18.
[6] S.R. White, N.R. Sottos, P.H. Geubelle, J.S. Moore, M.R. Kessler, S.R. Sriram, E.N. Brown, S. Viswanathan, Autonomic healing of polymer composites, Nature 409 (2001) 794–797.
[7] D.Y. Zhu, M.Z. Rong, M.Q. Zhang, Self-healing polymeric materials based on microencapsulated healing agents: from design to preparation, Prog. Polym. Sci. 49 (2015) 175–220.
[8] Y. Zhou, Y. Yan, Y. Du, J. Chen, X. Hou, J. Meng, Preparation and application of melamine-formaldehyde photochromic microcapsules, Sens. Actuators, B 188 (2013) 502–512.
[9] B.D. Credico, G. Griffini, M. Levi, S. Turri, Microencapsulation of a UV-responsive photochromic dye by means of Novel UV-Screening polyurea-based shells for smart coating applications, ACS Appl. Mater. Inter. 5 (2013) 6628–6634.
[10] M. De Bastiani, M.I. Saidaminov, I. Dursun, L. Sinatra, W. Peng, U. Buttner, O.F. Mohammed, O.M. Bakr, Thermochromic perovskite inks for reversible smart window applications, Chem. Mater. 29 (2017) 3367–3370.
[11] A.K. Mishra, B.B. Lahiri, J. Philip, Superior thermal conductivity and photo-thermal conversion efficiency of carbon black loaded organic phase change material, J. Mol. Liq. 285 (2019) 640–657.
[12] A.K. Mishra, B. Lahiri, V. Solomon, J. Philip, Nano-inclusion aided thermal conductivity enhancement in palmitic acid/di-methyl formamide phase change material for latent heat thermal energy storage, Thermochim. Acta 678 (2019) 178309.
[13] M. Zhao, C. Gao, F. Wang, K. Kuklane, I. Holmér, J. Li, The torso cooling of vests incorporated with phase change materials: a sweat evaporation perspective, Text. Res. J. 83 (2013) 418–425.
[14] A. Fonseca, T.S. Mayor, J.B.L.M. Campos, Guidelines for the specification of a PCM layer in Firefighting Protective Clothing Ensembles, Appl. Therm. Eng. 133 (2018) 81–96.
[15] A. Shaid, L. Wang, S.M. Fergusson, R. Padhye, Effect of aerogel incorporation in PCM-containing thermal liner of firefighting garment, Clothing Text. Res. J. 36 (2018) 151–164.
[16] X. Wan, F. Wang, Numerical analysis of cooling effect of hybrid cooling clothing incorporated with phase change material (PCM) packs and air ventilation fans, Int. J. Heat Mass Transf. 126 (2018) 636–648.
[17] H. Phelps, H. Sidhu, A mathematical model for heat transfer in fire fighting suits containing phase change materials, Fire Saf. J. 74 (2015) 43–47.
[18] H. Zhang, G. Song, H. Su, H. Ren, J. Cao, An exploration of enhancing thermal protective clothing performance by incorporating aerogel and phase change materials, Fire Mater. 41 (2017) 953–963.
[19] F. Zhu, Q. Feng, R. Liu, B. Yu, Y. Zhou, Enhancing the thermal protective performance of firefighters' protective fabrics by incorporating phase phange materials, Fibres Text. East. Eur. 23 (2015) 68–73.
[20] X. Geng, W. Li, Y. Wang, J. Lu, J. Wang, N. Wang, J. Li, X. Zhang, Reversible thermochromic microencapsulated phase change materials for thermal energy storage application in thermal protective clothing, Appl. Energy 217 (2018) 281–294.
[21] B. Peng, G. Huang, P. Wang, W. Li, W. Chang, J. Ma, C. Li, Effects of thermal conductivity and density on phase change materials-based thermal energy storage systems, Energy 172 (2019) 580–591.
[22] J. He, Y. Lu, Y. Chen, J. Li, Investigation of the thermal hazardous effect of protective clothing caused by stored energy discharge, J. Hazard. Mater. 338 (2017) 76.
[23] G. Song, F. Gholamreza, W. Cao, Analyzing thermal stored energy and effect on protective performance, Text. Res. J. 81 (2011) 1124–1138.
[24] G. Song, S. Paskaluk, R. Sati, E.M. Crown, J.D. Dale, M. Ackerman, Thermal protective performance of protective clothing used for low radiant heat protection, Text. Res. J. 81 (2011) 311–323.
[25] J. He, J. Li, Analyzing the transmitted and stored energy through multilayer protective fabric systems with various heat exposure time, Text. Res. J. 86 (2016) 235–244.
[26] Y. Su, J. He, J. Li, Modeling the transmitted and stored energy in multilayer protective clothing under low-level radiant exposure, Appl. Therm. Eng. 93 (2015) 1295–1303.
[27] S.A. Kahn, J.H. Patel, C.W. Lentz, D.E. Bell, Firefighter burn injuries: predictable patterns influenced by turnout gear, J. Burn Care Res. 33 (2012) 152–156.
[28] A.R. Moritz, F.C. Henriques, Studies of Thermal Injury: II. The relative importance of time and surface temperature in the causation of cutaneous burns, Am. J. Pathol. 23 (1947) 695–720.
[29] Y. Su, R. Li, J. Yang, G. Song, J. Li, Effect of compression on contact heat transfer in thermal protective clothing under different moisture contents, Clothing Text. Res. J. 38 (2020) 19–31.
[30] J.R. Lawson, W.H. Twilley, Development of an apparatus for measuring the thermal performance of fire fighters' protective clothing, US Department of Commerce, Technology Administration, National Institute of …, 1999.